MR Physics for Physicists:
Descerning Electric Properties & Electric Field Distributions from MR Images

Ulrich Katscher (ulrich.katscher@philips.com)
Philips Research Europe – Hamburg, Röntgenstrasse 24, 22335 Hamburg, Germany

Highlights

- Electric properties (i.e., permittivity and electric conductivity) of tissue can be determined quantitatively *in vivo* by suitable post-processing of transmit and/or receive RF coil sensitivities.
- As initial clinical application of this technique, a potential correlation between conductivity and malignancy of brain/breast tumors is currently investigated in several studies.
- Moreover, a suitable post-processing of transmit and/or receive RF coil sensitivities allows the estimation of electric fields, enabling a patient-individual estimation of local SAR.

Target audience

- Radiologists, scientists, and clinicians interested in new MRI contrasts as well as in new concepts in RF safety management

Outcome/objectives

- Participants will learn about the background, challenges, and applications of mapping tissue electric properties, as well as the possibility to experimentally estimate local SAR.

Purpose

The electric properties of human tissue, i.e., the electric conductivity σ and permittivity ε, can be used as additional diagnostic parameters or might be helpful for the prediction of the local SAR during MR measurements. "Electric Properties Tomography" (EPT) derives the patient's electric properties using a standard MR system, measuring the spatial transmit (TX) and/or receive (RX) sensitivity distribution of the applied RF coil(s) [1-8]. Thus, EPT does not apply externally mounted electrodes, currents, or RF probes, as is the case in competing techniques. EPT is quantitative MRI, i.e., it yields absolute values of σ and ε. Phantom experiments have proven the principle feasibility of EPT, and volunteer measurements underline its *in vivo* feasibility. Clinical studies have been started with preliminary, encouraging results.

Electric Properties – Background

The complex permittivity $\kappa = \varepsilon - i\sigma/\omega$ at an angular frequency ω can be probed by the time-harmonic magnetic field $\mathbf{H}$ via the Helmholtz equation (1). Particularly, κ can be estimated from the circularly polarized field component $H^+=|H^+|\exp(i\phi^+)$ (associated with the TX coil sensitivity) via Eqs. (2,3) using the following assumptions: (*i*) A locally ("piecewise") constant $\kappa(\mathbf{r})$, i.e. $\nabla\kappa(\mathbf{r}) = 0$. This "constant κ assumption" has severe consequences, which are discussed in the next section. (*ii*) A constant magnetic permeability $\mu(\mathbf{r}) = \mu_0$ and (*iii*) an isotropic κ. Both assumptions (*ii*) and (*iii*) are fairly fulfilled for human tissue at Larmor frequency. - To the leading order, the conductivity response affects the phase of H^+, while the permittivity response affects the magnitude of H^+. Thus, σ can be estimated by Eq. (4) based only on ϕ^+ ("phase-based conductivity imaging"). Accordingly, ε can be

$$-\Delta\mathbf{H} = \frac{\nabla\kappa}{\kappa}\times\left[\nabla\times\mathbf{H}\right] + \mu\omega^2\kappa\mathbf{H} \qquad (1)$$

$$\sigma(\mathbf{r}) = \frac{1}{\mu_0\omega}\,\mathrm{Im}\left\{\frac{\Delta H^+(\mathbf{r})}{H^+(\mathbf{r})}\right\} \qquad (2)$$

$$\varepsilon(\mathbf{r}) = -\frac{1}{\mu_0\omega^2}\,\mathrm{Re}\left\{\frac{\Delta H^+(\mathbf{r})}{H^+(\mathbf{r})}\right\} \qquad (3)$$

$$\sigma(\mathbf{r}) = \frac{\Delta\varphi^+(\mathbf{r})}{\mu_0\omega} \qquad (4)$$

$$\varepsilon(\mathbf{r}) = \frac{-\Delta\left|H^+(\mathbf{r})\right|}{\mu_0\omega^2\left|H^+(\mathbf{r})\right|} \qquad (5)$$

$$\mathrm{SAR}(\mathbf{r}) \sim \sigma(\mathbf{r})\mathbf{E}^2(\mathbf{r}) = \sigma(\mathbf{r})\left(\frac{\nabla\times\mathbf{H}(\mathbf{r})}{\omega\kappa(\mathbf{r})}\right)^2 \qquad (6)$$

estimated by Eq. (5) based only on $|H^+|$ ("magnitude-based permittivity imaging"). While $|H^+|$ can be measured directly via standard B_1 mapping techniques, ϕ^+ is more difficult to determine. The phase of a standard MR image ϕ_0 is always the superposition of ϕ^+ with its counterpart of the RF reception ϕ^-, and thus, is called "transceive phase". Using a quadrature volume coil, a rough approximation of ϕ^+ can be obtained by $\phi^+ \approx \phi_0/2$ ("transceive phase assumption"). On the other hand, the linearity of Eq. (4) supersedes the transceive phase assumption for phase-based conductivity imaging. Care has to be taken that the measured transceive phase is free of contributions unrelated to RF penetration, particularly free of off-resonance effects [1]. - A detailed description of the EPT background can be found in, e.g., [9].

Electric Properties – Challenges

As outlined above, the two central challenges of EPT are (A) the "constant κ assumption" and (B) the "transceive phase assumption". Several studies have been conducted to investigate these challenges [10-20], as summarized in the following.

Ad (A) "Constant κ Assumption": Neglecting spatial variations of κ (i.e., the first term on the right hand side of Eq. (1)) typically leads to strong over/undershooting of reconstructed κ along tissue boundaries [3]. The easiest way to avoid these boundary artefacts is to shape the size of the numerical differentiation kernel of Eqs. (2-5) to tissue boundaries, where discontinuous κ is expected [10,11]. Alternatively, boundary artefacts can be avoided by circumventing numerical differentiation via the EPT forward solution, i.e., iterating electric properties, until the resulting H^+ coincides with the observed H^+. This strategy has been realized by the Green's tensor-based „Contrast Source Inversion" method [12] and via solving the Poisson equation [13]. Yet another strategy is to solve the full Helmholtz equation (1). Missing information can be compensated, e.g., by comparison of different TX channels, which have to yield identical electric properties [4,14,15]. Neglecting spatial derivatives of H_z (e.g., by assuming a quadrature volume coil), Eq. (1) can be re-written as a function of H^+ only. The resulting equation can be solved by its transformation into a convection-reaction equation [16], or by an iteration calculating H^+ and E^+ alternately [17].

Ad (B) "Transceive Phase Assumption": TX and RX phase can be disentangled from the transceive phase in an exact, analytic manner by a comparison of different TX channels [18,14] in analogy to the constant κ assumption. Alternatively, Eqs. (2,3) can be re-written for ratios of different RX coils [19]. This H^--based EPT circumvents the transceive phase assumption, and has the additional advantage that – in contrast to multi-TX scans – it can be performed in a single scan. Unfortunately, the introduction of image ratios is equivalent with an additional differentiation [19], thus further deteriorating SNR of the reconstruction result. The transceive phase assumption can also be circumvented by re-writing Eqs. (2,3) as function of $\sqrt{(H^+ H^-)}$ [20]. To this goal, additional assumptions are required, which, according to [20], are less severe than the transceive phase assumption.

Electric Properties – Evaluation and Applications

Evaluating phantoms with different conductivities (adjusted via, e.g., NaCl concentration) and permittivities (adjusted via, e.g., alcohol concentration) covering the physiologic range yielded very high correlations between expected and measured σ and ε [2,3,21]. Furthermore, the brains of healthy volunteers have been investigated [5,6]. Values of σ and ε averaged over various brain compartments agree with literature values (see, e.g., [22]). The observed inter-subject variability of the mean σ and ε in the compartments mentioned is of the order of 10-20% [5].

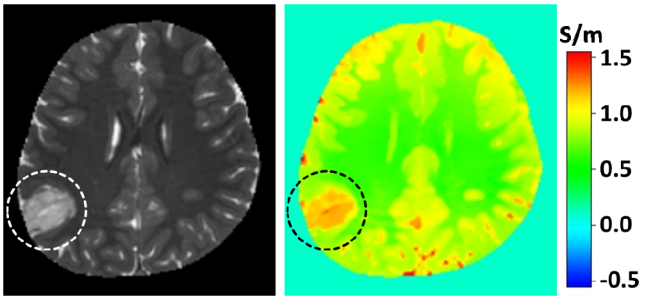

Fig. 1: Example of brain tumor conductivity map (9 yr. old boy with dysembryoplastic neuroepithelial tumor [26]). Left: SSFP magnitude image, right: conductivity map derived from SSFP phase image.

Results for brain tumors have been reported for 1.5 T, 3 T, and 7 T [23-25], always showing a significantly increased tumor conductivity compared with normal white matter (see Fig. 1). A correlation between brain tumor grade and conductivity has been found in [26]. A stroke patient was described by [27], showing again a clear increase of the conductivity within the stroke area. Applying EPT to mammography is more challenging than applying EPT to the brain due to typically highly nested gland and fat, which yields a particular challenge for the "constant κ assumption" discussed above. Nevertheless, a correlation between malignancy and conductivity has also been found for breast tumors [28,29]. It has been hypothesized that the biochemical reason for the observed pathologic conductivity alteration is predominantly given by an increased sodium concentration in tumors [30]. An EPT study of pelvic tumors is in preparation [31].

Electric Field Distributions / Local SAR

In analogy to the derivation of electric *properties* by post-processing TX/RX coil sensitivities, it has been investigated to also derive electric *fields* by post-processing TX/RX coil sensitivities. This technique would open the possibility to estimate local SAR by patient-individual measurements ("B_1-based SAR determination", BBS), in contrast to the model-based SAR determination usually applied in clinical MRI. In a first step, κ has to be determined as described above. In a second step, a model for the missing field component H_z has to be chosen. Last, the electric field is derived via Ampere's law and local SAR calculated according to Eq. (6). This technique has been applied for quadrature RF excitation [3,32] as well as for single rods of volume coils in the framework of parallel TX [18,33,34]. Example results for this procedure, applied to human thighs, are shown in Fig. 2. BBS is of particular interest for local surface coils, where standard model-based SAR estimation is hampered by the large number of degrees of freedom [36]. – Electric fields are also a byproduct of the above-mentioned EPT forward solution [12], and thus, can be used for BBS.

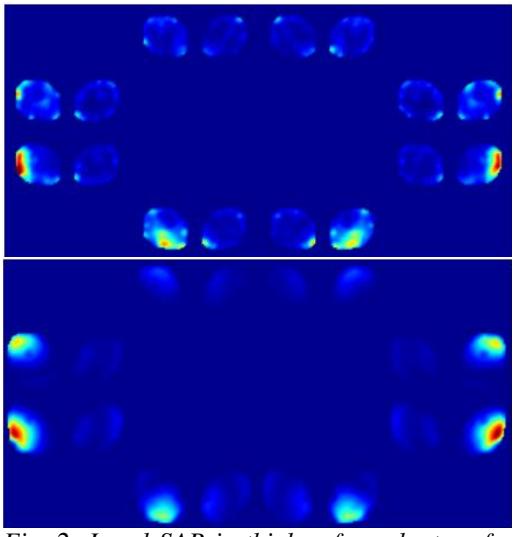

Fig. 2: Local SAR in thighs of a volunteer for eight single rods of a TX RF volume coil [35]. Above: Experimental EPT results, below: FDTD simulated results, based on the segmented 3D MR image of the individual volunteer shown above.

Summary / Conclusion

Using standard MR systems and standard MR sequences, mapping of tissue electric properties appears to be feasible clinically, particularly phase-based conductivity imaging. The rapidly evolving field will certainly afford further improved measurement and reconstruction techniques in the near future. The broad spectrum of clinical studies started raise hope that answers will soon be available concerning potential diagnostic benefits of EPT. Last but not least, EPT could open a new chapter in RF safety management by direct local SAR measurements, potentially superseding the hitherto applied simplifying generic SAR models.

References

[1] Haacke EM et al., Phys Med Biol 1991;36:723
[2] Wen H. Proc. SPIE 2003;5030:471
[3] Katscher U et al., IEEE Trans Med Imag. 2009;28:1365
[4] Zhang X et al., IEEE Trans Med Imag. 2010;29:474
[5] Voigt T et al., MRM 2011;66:456
[6] van Lier AL et al., MRM 2012;67:552
[7] Seo JK et al., IEEE Trans Med Imag 2012;31:430
[8] Bulumulla SB et al., Conc in Magn Reson Part B 2012;41B:13
[9] Katscher U et al., CMMM 2013;546562
[10] Katscher U et al., ISMRM 2012;20:3482
[11] Huang L et al., ISMRM 2014;22:3190
[12] Balidemaj E et al., ISMRM 2013;23:4185
[13] Borsic A et al, ISMRM 2014;22:3191
[14] Sodickson D et al., ISMRM 2012;20:387
[15] Liu J et al., ISMRM 2013;21:463
[16] Hafalir FS et al., ISMRM 2013;21:4187
[17] Lee JS et al., ISMRM 2013;21:4183
[18] Katscher U et al., MRM 2012;68:1911
[19] Marques JP et al., MRM, e-publication August 2014
[20] Lee SK et al., IEEE Trans Med Imag 2015;34:541
[21] Katscher U et al., ISMRM 2010;18:239.
[22] Gabriel S et al., Phys Med Biol. 1996;41:2251
[23] Voigt T et al., ISMRM 2012;19:127
[24] Huhndorf M et al., ISMRM 2013;21:3626
[25] van Lier AL et al., ISMRM 2011;19:4464
[26] Tha KK et al., ISMRM 2014;22:1885
[27] van Lier AL et al., ISMRM 2012;20:3484
[28] Katscher U et al., ISMRM 2013;21:3372
[29] Shin JW et al., JMRI, e-publication November 2014
[30] van Lier AL et al., ISMRM 2013;21:115
[31] Balidemaj E et al., MRM, e-publication April 2014
[32] Cloos MA et al., ISMRM 2009;17:3037.
[33] Buchenau S et al., Magn Reson Mater Phy 2013;26:463
[34] Zhang X et al., IEEE Trans Med Imag 2013;32:1058
[35] Katscher U et al., ISMRM 2012;20:2733
[36] Braun M et al., ISMRM 2015;23:3594